Journal of Medicinal Chemistry Article

J. Med. Chem. **2010,** *53,* 1117–1127 **1117**
DOI: 10.1021/jm901381j

Multifunctional Antioxidants for the Treatment of Age-Related Diseases

Hongxia Jin, James Randazzo, Peng Zhang, and Peter F. Kador*

College of Pharmacy, University of Nebraska Medical Center, Omaha, Nebraska 68198

Received September 17, 2009

Analogues of *N*,*N*-dimethyl-4-(pyrimidin-2-yl)piperazine-1-sulfonamide possessing a free radical scavenger group (FRS), chelating groups (CHL), or both (FRS + CHL) have been synthesized. Electrospray ionization mass spectrometry studies indicate that select members of this series bind ions in the relative order of $Cu^{1+} = Cu^{2+} > Fe^{2+} = Fe^{3+} > Zn^{2+}$ with no binding of Ca^{2+} or Mg^{2+} observed. In vitro evaluation of these compounds in human lens epithelial, human retinal pigmented epithelial, and human hippocampal astrocyte cell lines indicates that all analogues possessing the FRS group as well as the water-soluble vitamin E analogue 6-hydroxy-2,5,7,8-tetramethylchroman-2-carboxylic acid protect these cells against decreased cell viability and glutathione levels induced by hydrogen peroxide. In addition, those compounds possessing CHL groups also protected these cells against hydroxyl radicals generated by the Fenton reaction. These compounds are good candidates for the preventive treatment of cataract, age-related macular degeneration (AMD), and Alzheimer's dementia (AD).

Introduction

Oxidative stress damages cells and is an accepted determinant of both lifespan and health span. Oxidative stress results from the generation of reactive oxygen species (ROS[a]), primarily H_2O_2, and is enhanced by the age-related decrease of cellular antioxidant defenses and accumulation of iron and/or copper.[1] The increased cellular presence of these redox-active metals enhance H_2O_2-linked ROS by generating hydroxyl radicals through the Fenton reaction.[2,3] Age-related increases in ROS are believed to trigger biochemical cascades that lead to neurodegenerations such as AD,[4−6] retinal degenerations such as age-related macular degeneration (AMD),[7−10] and cataract formation.[7,11] While these diseases are pathologically different, studies suggest that they all undergo similar oxidative damage from ROS associated with redox-active metal ions. For example, ROS-associated Aβ in amyloid plaques, which are characteristic of AD,[4,12−15] is also present in AMD[16−18] and age-related cataract.[19−21]

The oxidative pathways associated with neurodegenerations and age-related ocular diseases have been targeted as a potential therapeutic approach to the treatment of these age-related diseases.[5] A wide variety of antioxidants have been examined to reduce ROS. These range from natural products with antioxidant properties such as aged garlic extract, curcumin, melatonin, resveratrol, *Ginkgo biloba* extract, green tea, vitamin C, L-carnosine, vitamin E, and cannabinoids to derivatives of lipoic acid, analogues of coenzyme Q (MitoQ), and "thiol-delivering" glutathione mimics such as tricyclodecan-9-yl xanthogenate.[22−29] Some of these agents have shown limited clinical efficacy with AMD,[30,31] but none have demonstrated clinical efficacy in reducing the clinical signs of neurodegeneration or cataract.

Reducing ROS through the chelation of redox-active metals is another approach that has been investigated; however, this approach has primarily been used to treat neurodegenerations. Examples are illustrated in Figure 1. Of these compounds, only the iron chelator desferrioxamine (DFO, *N*′-{5-[acetyl(hydroxy)amino]pentyl}-*N*-[5,4- [(5-aminopentyl)-(hydroxy)amino]-4-oxobutanoyl}amino)pentyl]-*N*-hydroxysuccinamide) and clioquinol (5-chloro-7-iodoquinolin-8-ol) has been investigated for both neurological[32,33] and age-related ocular diseases.[34−36] Desferrioxamine is not orally active and does not significantly cross the blood−brain barrier.[37,38] Clioquinol is an orally active antibiotic that was extensively used as an antibiotic in Asia in the 1960s. In 1971 it was banned in Japan after being linked to subacute myelo-optic neuropathy (SMON) in over 10 000 Japanese people. Its chelating ability was subsequently identified during neurotoxicity studies[39] where it has been demonstrated to decrease Cu uptake and counteract Cu efflux activities of the amyloid precursor protein of AD,[40] disaggregate the metal ion-induced aggregates of Aβ(1−40), and retard fibril growth through a Zn(II) clioquinol complex formation.[41] Its efficacy has been demonstrated in vitro, in in vivo animal models, and in several small clinical trials of AD patients.[15,42,43] Because of the promising results of clioquinol, several other 8-hydroxyquinoline analogues have been developed: PBT2 (structure not disclosed to date),[44,45] M-30 (5-((methyl(prop-2-ynyl)-amino)methyl)quinolin-8-ol),[46,47] VK-28 5-((4-(2-hydroxyethyl)-piperazin-1-yl)methyl)quinolin-8-ol),[46] HLA-20 (5-((4-(prop-2-ynyl)piperazin-1-yl)methyl)quinolin-8-ol),[46] deferasirox (4-(3,5-bis(2-hydroxyphenyl)-1*H*-1,2,4-triazol-1-yl)benzoic acid),[46−48] deferiprone (3-hydroxy-1,2-dimethylpyridin-4(1*H*)-one),[49] feralex (2-(3-hydroxy-2-methyl-4-oxo-3,4-dihydropyridin-1(2*H*)-yl)-*N*-((3*R*,4*R*,5*S*,6*R*)-2,4,5-trihydroxy-6-(hydroxylmethyl)-tetrahydro-2*H*-pyran-3-yl)acetamide,[50,51] D-penicillamine ((*S*)-2-amino-3-mercapto- 3-methylbutanoic acid),[52]

*To whom correspondence should be addressed. Phone: 402-559-9261. Fax: 402-559-9543. E-mail: pkador@unmc.edu.

[a] Abbreviations: AD, Alzheimer's dementia; AMD, age-related macular degeneration; BSA, bovine serum albumin; CHL, chelating groups; FRS, free radical scavenger groups; hLECs, human lens epithelium cells; HA-h, human hippocampal astrocytes; ROS, reactive oxygen; SDI, sorbitol dehydrogenase inhibitor.

Published on Web 01/15/2010

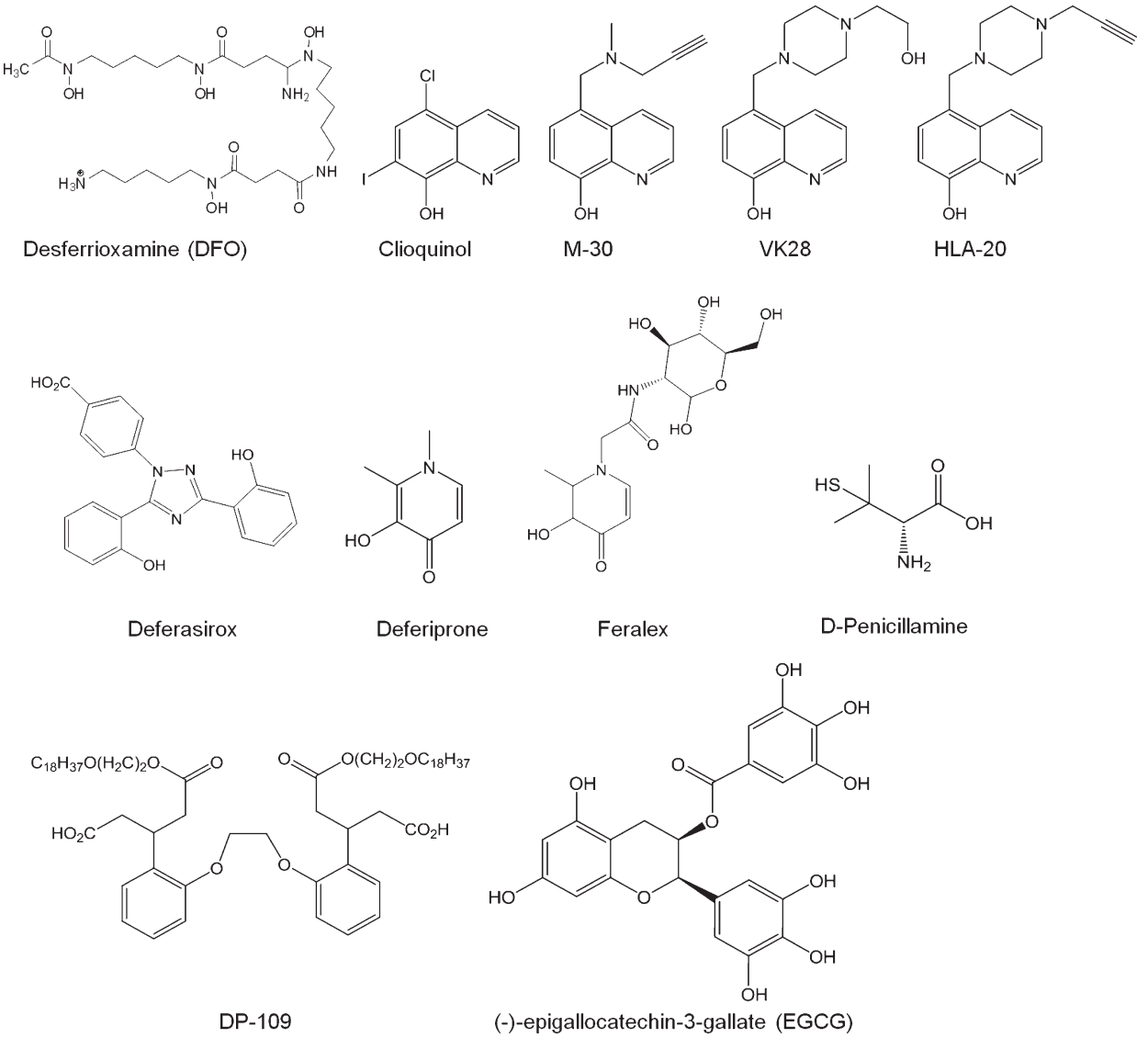

Figure 1. Structure of antioxidant and chelators evaluated for cataract, AMD, and AD.

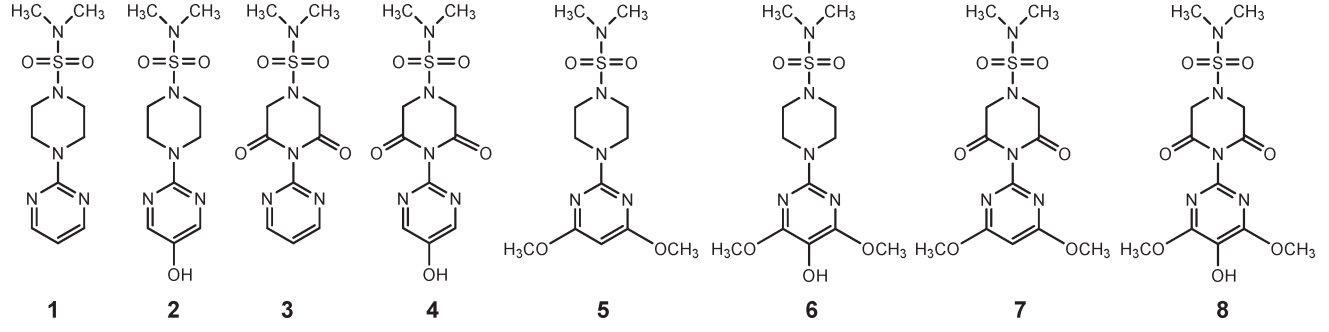

Figure 2. Analogues of *N*,*N*′-dimethyl-4-(pyrimidin-2-yl)piperazine-1-sulfonamide (**1**) synthesized and evaluated.

DP-109 (3,3′-(2,2′-(ethane-1,2-diylbis(oxy))-bis(2,1-phenylene))-bis(5-(2-(octadecyloxy)ethoxy)-5-oxopentanoic acid),[53] and (−)-epigallocatechin 3-gallate (EGCG) ((2*R*,3*R*)-5,7-dihydroxy-2-(3,4,5-trihydroxyphenyl)chroman-3-yl-3,4,5-trihydroxybenzoate).[54]

To date, many research efforts on the treatment of ROS-linked complications have focused on therapeutic targets that enhance cellular antioxidant defenses, demonstrate antioxidant activity, or regulate cellular levels of transition metal ions.[43,55] Because multiple mechanisms are involved in the development of ROS-linked disorders, drugs with at least two mechanisms of action targeted at ROS may offer more therapeutic benefit than those only targeting a single mechanism. Toward this end, we have synthesized a series of multifunctional analogues of *N*,*N*-dimethyl-4-(pyrimidin-2-yl)-piperazine-1-sulfonamide (**1**) (Figure 2) possessing a FRS group, (analogues **2**, **6**), CHL groups (CHL, analogues **3**, **7**), or both (analogues **4**, **8**).[56] The ring structure of the parent compound **1** was derived from studies investigating the effect

of sorbitol dehydrogenase inhibitors (SDI) on sugar cataract formation.[57] FRS activity was introduced to **1** by addition of an −OH group in the 5-position of the pyrimidine ring. This was based on a report that 5-pyrimidinols are more effective antioxidants than their corresponding phenols, with 2-*N*,*N*-dimethyl-4,6-dimethyl-5-hydroxypyrimidine being 5-fold more reactive toward alkyl radicals and essentially equally reactive to peroxy radicals compared to α-tocopherol.[58] Methoxy groups, rather than methyl groups, were added to the pyrimidine ring because methoxy groups stabilize the radical scavenger slightly better than the methyl groups and are not as readily subjected to metabolic oxidation as the methyl groups.[59−61] The ability to chelate was introduced by adding carbonyl groups directly adjacent to the amino group connecting the piperazine ring to the pyrimidine ring. This was based on a report that 2-*N*-succinamide-1,3-pyrimidine easily forms complexes with transition metals such as Fe^{3+} and Cu^{2+}.[62]

Scheme 1[a]

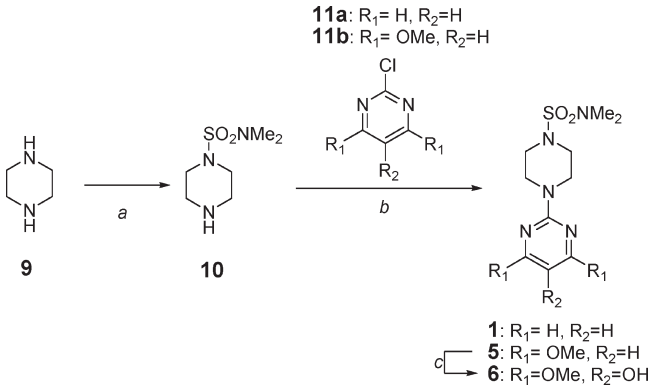

[a] Reagents and conditions: (a) $ClSO_2NMe_2$, K_2CO_3, EtOH, room temperature; (b) TEA, THF, reflux; (c) *n*-BuLi, THF, O_2, −78 °C to room temperature.

Chemistry

Compounds **1**, **5**, and **6** were synthesized as outlined in Scheme 1. *N*,*N*-Dimethylpiperazine-1-sulfonamide **10** was obtained from commercially available piperazine **9** according to the literature.[63] Nucleophilic substitution of 2-chloropyrimidines **11a** and **11b** with *N*,*N*-dimethylpiperazine-1-sulfonamide **10** gave **1** and **5**, respectively. Compound **6** was obtained through directed hydroxylation of **5**. The aromatic anion of **5**, which was generated in the presence of *n*-BuLi, was treated with oxygen gas to give **6**.[64]

The 5-hydroxypyrimidine analogue **2** was also initially obtained by nucleophilic substitution of 2-chloro-5-hydroxypyrimidine (**15**) with *N*,*N*-dimethylpiperazine-1-sulfonamide (**10**) (Scheme 2). Compound **15** was obtained from commercially available 2-chloro-5-nitropyrimidine (**12**) by first reducing the nitro group to 2-chloro-5-aminoprimidine (**13**) by refluxing with acetic acid in the presence of iron. Subsequent diazotization of the amine **13** failed; however, 2-chloro-5-hydroxypyrimidine **15** could be obtained in poor yield (33%) by refluxing **13** with 2 M sulfuric acid.[65]

Because of the poor yield in obtaining **15**, an alternative approach to compound **2** was employed. As outlined in Scheme 3, an initial nucleophilic reaction of *N*,*N*-dimethylpiperazine-1-sulfonamide **10** with 2-chloro-5-nitropyrimidine **12** gave the nitro product **16** which was reduced to the amine **17** by refluxing with NH_4Cl and iron. Refluxing amine **17** with 2 M sulfuric acid gave **2** in 56% yield.

The piperazine-2,6-dione containing analogues were synthesized by condensation of 2,2′-(*N*,*N*-dimethylsulfamoylazanediyl)diacetic acid (**19**), obtained from commercially available iminodiacetic acid (2,2′-azanediyldiacetic acid) (**18**), with primary aromatic amines **20a**−**d** (Scheme 4). The piperazine-2,6-diones **3**, **7**, **21**, and **22**, respectively, were obtained by activation of the 2,2′-(*N*,*N*-dimethylsulfamoyliminodiacetic acid (**19**) with acetic anhydride (step b), addition of **20a**−**d** (step c), and subsequent dehydration (step d).[66] The benzyl

Scheme 2[a]

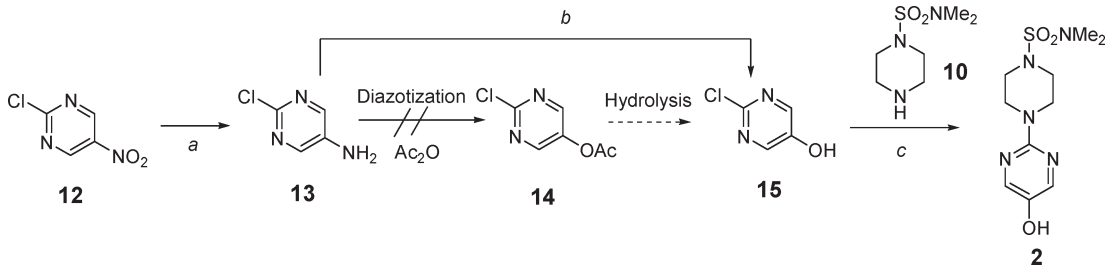

[a] Reagents and conditions: (a) Fe, AcOH, reflux; (b) 2 M H_2SO_4, reflux; (c) TEA, THF, reflux.

Scheme 3[a]

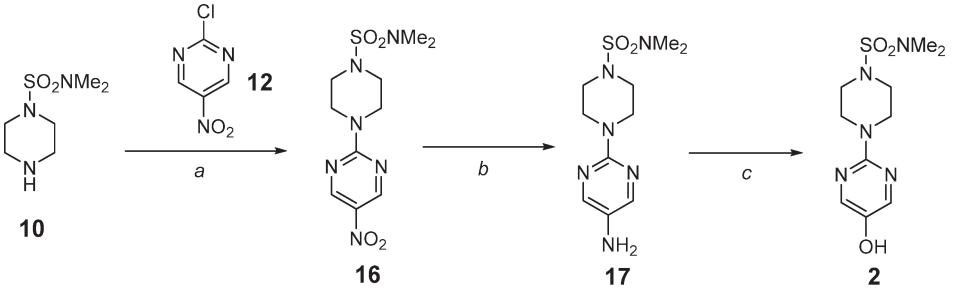

[a] Reagents and conditions: (a) TEA, THF, room temperature; (b) Fe, NH_4Cl, EtOH−H_2O, reflux; (c) 2 M H_2SO_4, reflux.

Scheme 4[a]

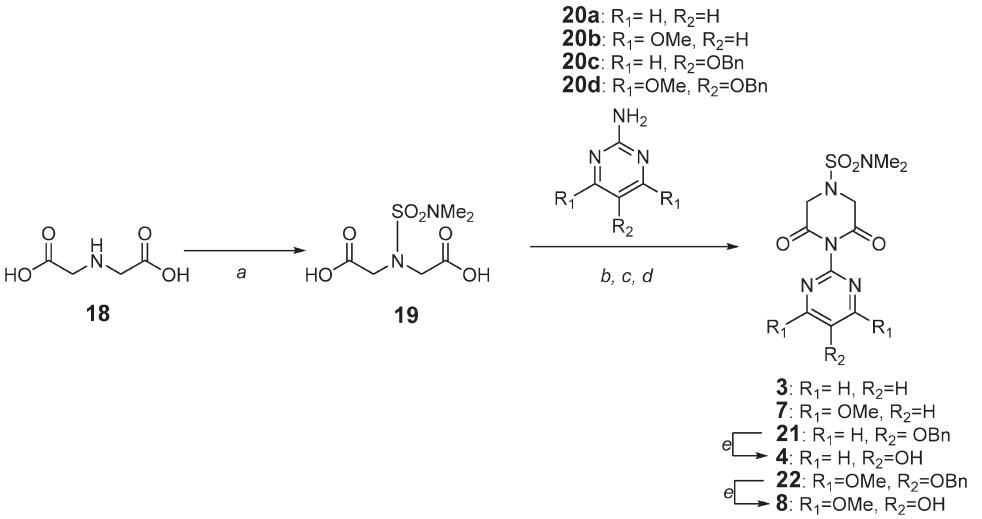

[a] Reagents and conditions: (a) $ClSO_2NMe_2$, NaOH, Na_2CO_3, acetone−H_2O, 0 °C to room temperature; (b) Ac_2O, 85 °C; (c) acetone, toluene, 80 °C; (d) Ac_2O, 80 °C; (e) Pd−C, H_2, EtOAc, room temperature.

Scheme 5[a]

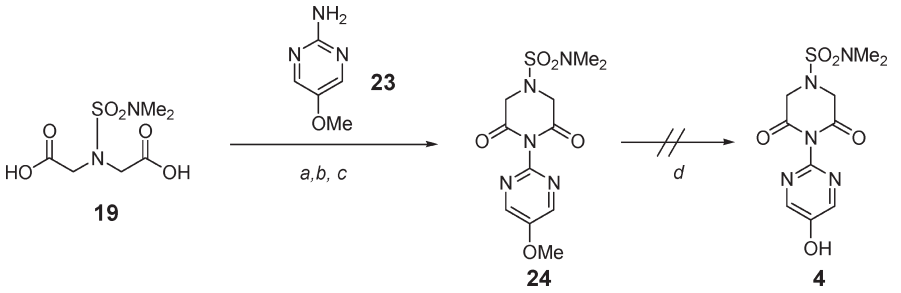

[a] Reagents and conditions: (a) Ac_2O, 85 °C; (b) acetone, toluene, 80 °C; (c) Ac_2O, 80 °C; (d) BBr_3, benzene, room temperature; or TMSI, $CHCl_3$; or MeCN.

protecting groups of **21** and **22** were removed by hydrogenolysis to give final **4** and **8**, respectively. Compounds **20a** and **20b** were commercially available.

To obtain compound **4**, the synthesis outlined in Scheme 5 was initially employed. The methoxy **24** was obtained in 60% yield in a three-step pot reaction from **19** and **23** according to published procedures.[67] However, attempts at selectively cleaving the methoxy group of **24** failed. In the presence of BBr_3, a number of cleavage products were obtained, presumably because of the instability of 2,6-dioxopiperazine in the presence of the strong Lewis acid. Alternatively, no reaction was observed with mild treatment of **24** with TMSI for 12 h. Condensation of **19** with 2-amino-5-hydroxypyrimidine, **25**, the cleaved methoxy product of **23**, also did not result in the anticipated amide **27** (Scheme 6). Instead, ester **26** was formed because the 5-hydroxyl group of 2-amino-5-hydroxypyrimidine, **25**, is more reactive; however, protection of the hydroxyl group with an easily removable benzyl group gave amine **20c** which when condensed yielded compound **21**. Subsequent hydrogenolysis of **21** gave the desired compound **4**.

2-Amino-5-(benzyloxy)-4,6-dimethoxypyrimidine (**20d**) was obtained from commercially available 2-chloro-4,6-dimethoxypyrimidine **11b** (Scheme 7). Oxidation of the aromatic anion of **11b** generated in the presence of dioxygen gave the hydroxyl **28** in 44% yield. This yield was increased to 94% when dioxygen was replaced with lithium *tert*-butyl peroxide which was generated in situ from *tert*-butylperoxy alcohol

Scheme 6

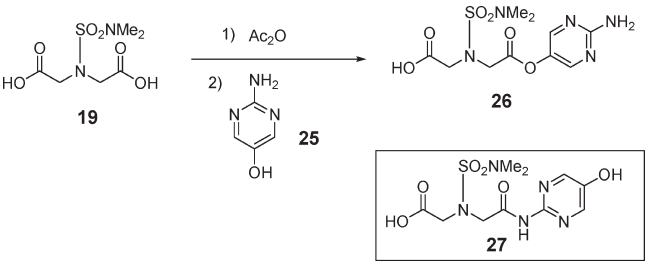

and *n*-butyllithium.[68] Following benzylation of the hydroxyl group, the 2-chlorine atom was replaced with an amino group. Attempted substitution of the chlorine with an ammonia−methanol solution or ammonia hydroxide was unsuccessful. Refluxing chloride **29** in toluene with benzylamine resulted in the formation of the 2-benzyllamine **30** in 33% yield and a 64% yield (according to the procedure for preparation of compound **30**) with 25% recovery of chloride **29**. Replacing toluene with dioxane increased the yield of **30** to 55% with 25% recovery of **29**. Attempted selective hydrogenolysis of **30** for 2 h at room temperature and 1 atm resulted in 2-benzylamino-4,6-dimethoxy-5-hydroxyprimidine in 90% yield and 2-amino-4,6-dimethoxy-5-hydroxyprimidine **31** in 10% yield. Both benzyl groups were removed to give **31** in 98% yield when hydrogenolysis was increased to 12 h. The benzyl group was

Scheme 7[a]

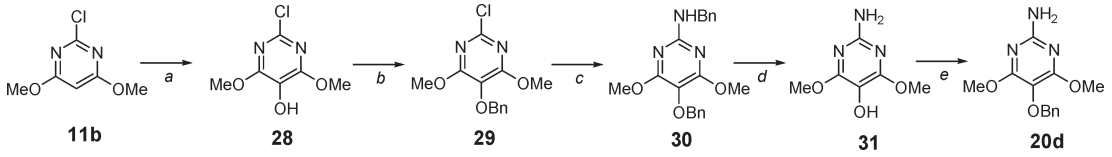

[a] Reagents and conditions: (a) LDA, *t*-BuOOLi, THF, −78 °C; (b) BnBr, K_2CO_3, MeCN, room temperature; (c) $BnNH_2$, K_2CO_3, dioxane, reflux; (d) Pd−C, H_2, MeOH, room temperature; (e) BnBr, K_2CO_3, MeOH, room temperature.

Table 1. Percent Parent Peaks Remaining at 10:1 Metal Ion Solution/Compound Obtained by ESI-MS

	% parent peaks in ion solutions						
compd	Fe^{2+}	Fe^{3+}	Cu^{1+}	Cu^{2+}	Zn^{2+}	Ca^{2+}	Mg^{2+}
1	100.0	100.0	100.0	100.0	100.0	100.0	100.0
2	100.0	100.0	100.0	100.0	100.0	100.0	100.0
3	8.1	10.0	3.6	4.4	15.3	100.0	100.0
4	6.9	8.2	4.2	3.0	12.7	100.0	100.0
5	100.0	100.0	100.0	100.0	100.0	100.0	100.0
6	100.0	100.0	100.0	100.0	100.0	100.0	100.0
7	7.3	7.6	4.1	3.4	13.8	100.0	100.0
8	7.5	8.2	4.0	3.6	14.6	100.0	100.0

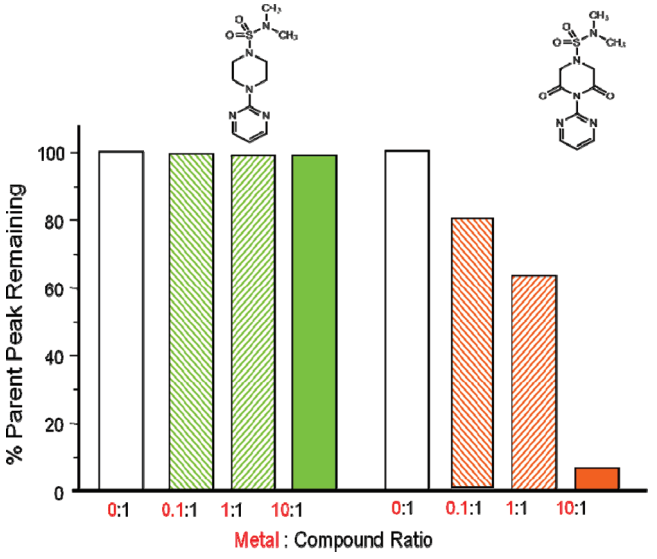

Figure 3. ESI-MS analysis of parent peak of *N*,*N*′-dimethyl-4-(pyrimidin-2-yl)piperazine-1-sulfonamide (**1**) and *N*,*N*′-dimethyl-3,5-dioxo-4-(pyrimidin-2-yl)piperazine-1-sulfonamide (**3**) in the presence of increasing amounts of Fe^{2+} solutions.

then reintroduced to the 5-hydroxy group to give **20d** under conditions similar to those employed for the synthesis of **20c**.

Chelation Studies. The relative amounts of Fe^{2+}, Fe^{3+}, Cu^{1+}, Cu^{2+}, Zn^{2+}, Ca^{2+}, Mg^{2+} ions bound by compounds **1**−**8** were determined by electrospray ionization mass spectrometry (ESI-MS) by mixing each ion solution with compound in molar ratios of 10:1, 1:1, and 1:10 and then directly infusing each solution under constant ionization energy. Table 1 summarizes the relative percent parent peak observed with a 10:1 metal ion/compound solution for each compound. Under these conditions, a relative decrease in compound parent peak height only occurs with increased ion binding. This is illustrated in Figure 3 where the parent peak heights of compounds **1** and **3** are compared. Only compound **3** which contains the necessary piperazine-2,6-dione groups required for ion binding shows a decrease in peak height with increasing concentration of Fe^{2+}. Ion

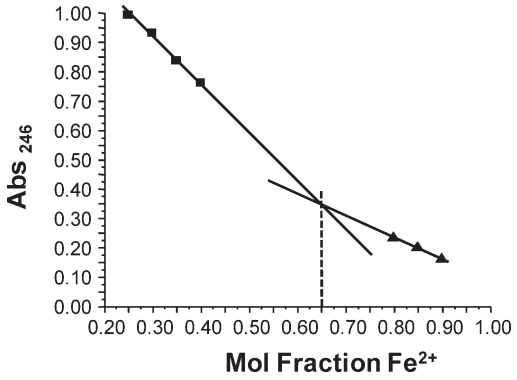

Figure 4. Job's plot of compound **4** in acetate solution (1 mM, pH 6.5) at 23 °C. The final concentration of compound **4** and Fe^{2+} ion was maintained constant at 0.1 mM.

Table 2. Stoichiometry of Metal Ion Binding to Compounds Obtained from Job Plots[a]

	stoichiometry in ion solutions						
compd	Fe^{2+}	Fe^{3+}	Cu^{1+}	Cu^{2+}	Zn^{2+}	Mg^{2+}	Ca^{2+}
1	0[b]	0[b]	0[b]	0[b]	0[b]	0[b]	0[b]
2	0[b]	0[b]	0[b]	0[b]	0[b]	0[b]	0[b]
3	2:1.06	2.101	1.212	1:2.03	1:1.94	0[b]	0[b]
4	2:1.08	2.096	1.194	1:1.99	1:2.08	0[b]	0[b]
5	0[b]	0[b]	0[b]	0[b]	0[b]	0[b]	0[b]
6	0[b]	0[b]	0[b]	0[b]	0[b]	0[b]	0[b]
7	2:1.08	2.099	1.194	1:1.99	1:1.86	0[b]	0[b]
8	2:1.10	2.099	1.190	1:2.08	1:1.99	0[b]	0[b]

[a] The total concentration of compound to metal ion was maintained at 0.1 mM. [b] Nonintersecting lines in the Job plot.

binding was only observed with compounds **3**, **4**, **7**, and **8** all of which possess the required piperazine-2,6-dione groups. These compounds bound ions with a relative binding order of $Cu^{1+} = Cu^{2+} > Fe^{2+} = Fe^{3+} > Zn^{2+}$. No binding was observed with either Ca^{2+} or Mg^{2+}.

To obtain the stoichiometry of the chelator−ion complexes, Jobs plots were prepared for compounds **1**−**8** with Fe^{2+}, Fe^{3+}, Cu^{1+}, Cu^{2+}, Zn^{2+}, Ca^{2+}, and Mg^{2+}. The maximum absorbance for each compound as a function of the mole fraction of the metal ion was determined and plotted to give linear dependences at high and low molar fractions. The stoichiometry of the formed complexes was determined by the intersections of these lines. The intersection of these lines corresponded to the stoichiometry of the complex formed (Figure 4). Intersecting lines were not observed with compounds **1**, **2**, **5**, or **6** or any compounds incubated with Ca^{2+} and Mg^{2+}; therefore, no stoichiometry could be obtained for these compounds or ions. This was consistent with the ESI-MS data. Binding stoichiometry for compounds **3**, **4**, **6**, and **7**, summarized in Table 2, was determined to be 1 metal chelator/2 metal ions for those ions with a tetrahedral/square planar geometry (Cu^{1+}, Cu^{2+}, Zn^{2+}) or to be 2 metal

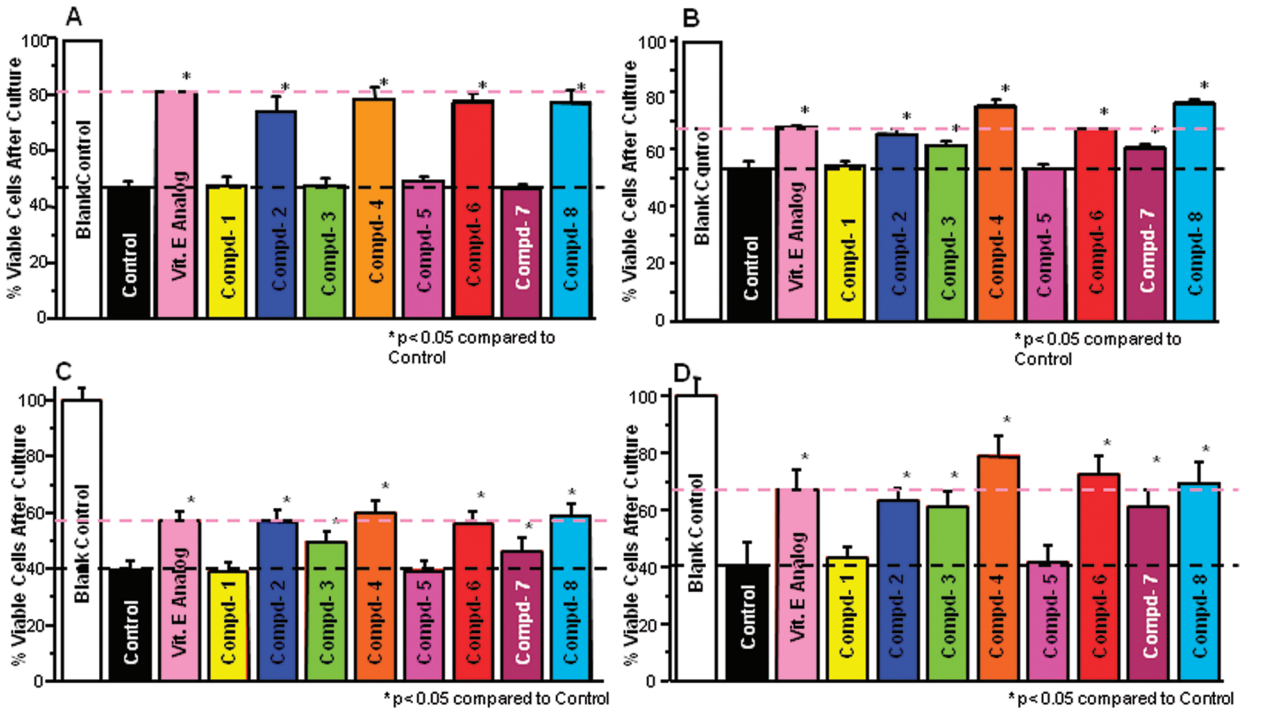

Figure 5. In vitro MTS viability assay of HLECs subjected to ROS. Part A illustrates exposure of HLECs exposed for 2 h with 1 mM H_2O_2 with/without the presence of the water-soluble vitamin E analogue 6-hydroxy-2,5,7,8-tetramethylchroman-2-carboxylic acid or compounds **1**−**8**. Part B illustrates 2 h exposure of HLECs with 1 mM Fenton's reagent with/without the presence of the vitamin E analogue or compounds **1**−**8**. Parts C and D illustrate similar 2 h exposure of hRPE and HA-h cells, respectively, with 1 mM Fenton's reagent with/without the presence of the vitamin E analogue or compounds **1**−**8**. All studies were normalized against MTS cell staining obtained without ROS (blank control), and the results represent the mean ± SD of three separate experiments. Significant differences ($p > 0.05$), calculated by ANOVA, were compared to control staining obtained with ROS in the absence of either the vitamin E analogue or compounds **1**−**8**.

chelators/1 metal ion for ions having an octahedral geometry (Fe^{2+}, Fe^{3+}). This stoichiometry was consistent with the data of a similar chelating moiety in 2-(*N*-succinimidyl) pyrimidine.[62]

In Vitro Evaluation of Antioxidant Activity. Compounds **1**−**8** were evaluated for their ability to protect SRA-1 human lens epithelium cells (hLECs),[69] commercially available ARPE-19 human retinal pigmented epithelial cells (RPEs),[70] and HA-h human hippocampal astrocytes (HA-hs). These three cells types are instrumental in the development of cataract, AMD, and AD, respectively.

In the first set of studies, the ability of compounds **1**−**8** to protect cells against ROS-induced cell death was evaluated using a MTS Cell Viability assay. The results were compared to the protective activity of the water-soluble vitamin E analogue 6-hydroxy-2,5,7,8-tetramethylchroman-2-carboxylic acid. All cells were exposed for 2 h of either 1.0 mM H_2O_2 or Fenton reagents (1.0 mM H_2O_2 and 1.0 mM Fe^{2+}) with/without 1 mM compounds **1**−**8** or 6-hydroxy-2,5,7,8-tetramethylchroman-2-carboxylic acid. As summarized in Figure 5A, the presence of H_2O_2, reduced the viability of the hLECs to less that 50%. A similar loss of cell viability was observed for compounds **1**, **3**, **5**, and **7**, analogues not possessing the 2-amino-5-hydroxy-1,3-pyrimidine group required for FRS activity. 6-Hydroxy-2,5,7,8-tetramethylchroman-2-carboxylic acid significantly protected cell viability against ROS, and similar protection was also observed with compounds **2**, **4**, **6**, and **8**; all compounds possess the 2-amino-5-hydroxy-1,3-pyrimidine FRS group. When ROS was generated by the Fenton reaction (Figure 5B), in addition to the FRS containing compounds **2**, **4**, **6**, and **8**, some protection was now also demonstrated with compounds **3** and **7** which contain the 2,8-dioxopiperazine CHL group. Moreover, the multifunctional compounds possessing both FRS and CHL groups (compounds **4** and **8**) demonstrated better protection than 6-hydroxy-2,5,7,8-tetramethylchroman-2-carboxylic acid. Similar results were observed for the RPE and HA-h cells. The protection afforded by compounds **1**−**8** against Fenton's reagent is summarized in Figure 5C and Figure 5D, respectively.

In these three cell types, the rapid intracellular reduction of cellular glutathione (GSH) is a sensitive marker of oxidative stress. As illustrated in Figure 6A, the presence of 1 mM H_2O_2 rapidly resulted in a reduction of GSH levels in hLECs and a similar reduction was also observed with compounds **1**, **3**, **5**, and **7**, analogues not possessing the FRS group. However, GSH levels were maintained when similar cells were treated with either the water-soluble vitamin E analogue 6-hydroxy-2,5,7,8-tetramethylchroman-2-carboxylic acid or compounds **2**, **4**, **6**, and **8** which possess the FRS group. All compounds possess the 2-amino-5-hydroxy-1,3-pyrimidine FRS group. With Fenton generated ROS (Figure 6B), protection was also afforded by the CHL containing compounds **3** and **7**. In addition, the multifunctional compounds possessing both FRS and CHL groups (compounds **4** and **8**) demonstrated slightly better protection than 6-hydroxy-2,5,7,8-tetramethylchroman-2-carboxylic acid. Again, similar results were observed for the RPE and HA-h cells. The protection afforded by compounds **1**−**8** against Fenton's reagent is summarized in Figure 6C and Figure 6D, respectively.

Experimental Section

NMR spectra were obtained with a Varian 500 MHz spectrometer. EI-MS utilized an Agilent 5973N MSD, and ESI-MS was conducted with a Finnigan MAT LCQ. UV−visible spectra were

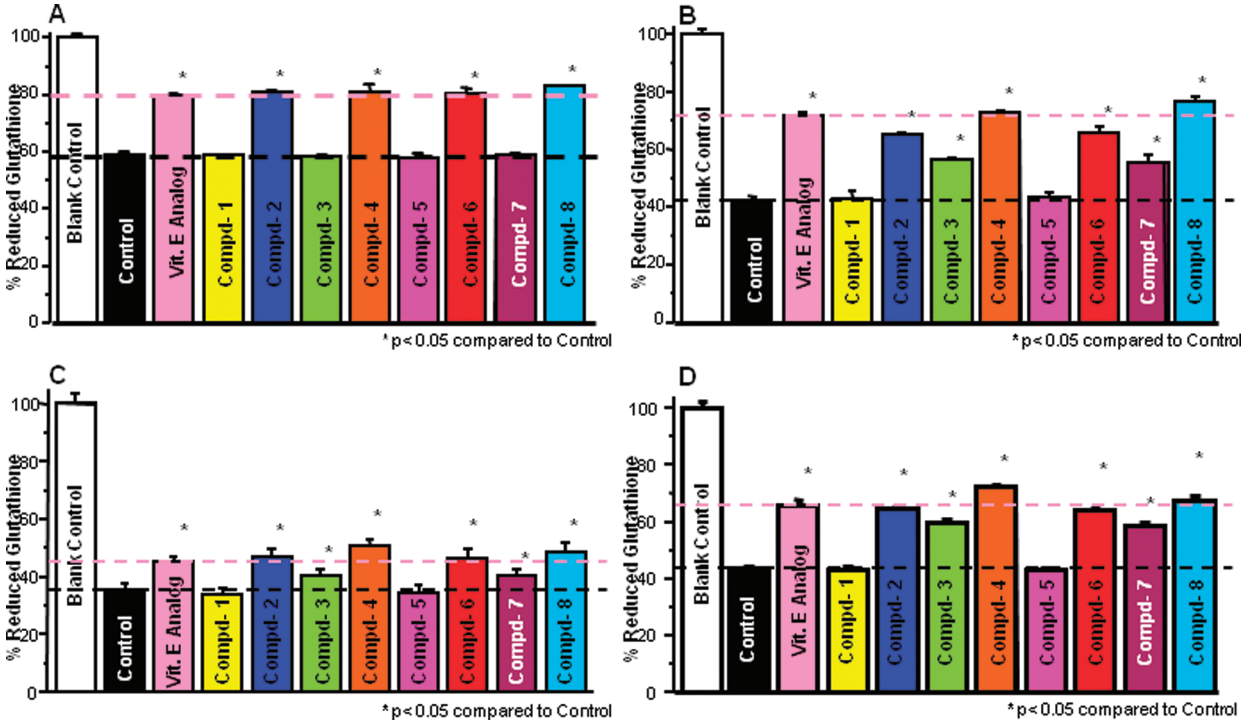

Figure 6. GSH levels in in vitro cells subjected to ROS. Part A illustrates exposure of HLECs exposed for 2 h with 1 mM H_2O_2 with/without the presence of the water-soluble vitamin E analogue 6-hydroxy-2,5,7,8-tetramethylchroman-2-carboxylic acid or compounds **1**−**8**. Part B illustrates 2 h exposure of HLECs with 1 mM Fenton's reagent with/without the presence of the vitamin E analogue or compounds **1**−**8**. Parts C and D illustrate similar 2 h exposure of hRPE and HA-h cells, respectively, with 1 mM Fenton's reagent with/without the presence of the vitamin E analogue or compounds **1**−**8**. GSH levels were expressed as nmol of GSH/mg of protein, with values normalized to GSH levels in cells not exposed to H_2O_2 (blank control, 100%). The results represent the mean ± SD of three separate experiments. Significant differences ($p > 0.05$), calculated by ANOVA, were compared to control staining obtained with ROS in the absence of either the vitamin E analogue or compounds **1**−**8**.

measured on a Molecular Devices SpectraMax Plus^{384} microplate spectrophotometer (Molecular Devices, Sunnyvale, CA). Melting points were uncorrected. Column chromatography (CC) utilized Merck silica gel (230−400 mesh). Final compound purities were assessed as ≥99% and intermediate compound purities were assessed as ≥96% by reverse phase HPLC using a 250 mm × 4.6 mm C18 Luna column (5 μ100 Å) with a mobile phase of 75:25 methanol/water at a flow rate of 0.9 mL/min and detection at 220, 254, and 280 nm. Elemental analyses were performed by M-H-W Laboratories, Phoenix, AZ.

***N,N′*-Dimethylsulfamoylpiperazine (10).** **1** was obtained according to the literature.[63]

General Procedure for the Preparation of *N,N′*-Dimethyl-4-(pyrimidin-2-yl)piperazine-1-sulfonamide (1) and 4-(4,6-dimethoxypyrimidin-2-yl)-*N,N′*-Dimethylpiperazine-1-sulfonamide (5). Et_3N (0.73 mL, 5.2 mmol) was added to 1.0 g of *N,N′*-dimethylsulfamoylpiperazine **10** (5.2 mmol) dissolved in 20 mL of THF. 2-Chloro-4,6-dimethoxypyrimidine **11a** (0.9 g, 5.2 mmol) dissolved in 5 mL of THF was then added, and the mixture was refluxed with stirring for 40 h. After the mixture was cooled, THF was removed under vacuum and the remaining yellow solid was dissolved in 300 mL of $CHCl_3$, washed with 0.5 N HCl, water, and brine, dried over Na_2SO_4, and filtered. Removal of solvent and CC with 1:1 $CHCl_3$/hexane gave 1.4 g (81%) of white compound **1**, mp 157−158 °C. ^{1}H NMR ($CDCl_3$) δ 8.34 (s, 1H), 8.33 (s, 1H), 6.55 (t, J = 4.88 Hz, 1H), 3.92 (appt, J = 5.13 Hz, 4H), 3.31 (appt, J = 5.13 Hz, 4H), 2.86 (s, 6H); ^{13}C NMR ($CDCl_3$) 161.4, 157.3, 110.5, 46.1, 43.4, 38.2; ESI-MS (m/z) 294 ($[M + Na]^+$). Anal. Calcd for $C_{10}H_{17}N_5O_2S$: C, 44.26; H, 6.31; N, 25.81; S, 11.82. Found: C, 44.12; H, 6.42; N, 25.58; S, 12.03. The yield of compound **5**, mp 103−105 °C, was 81%. ^{1}H NMR ($CDCl_3$) δ 5.41 (s, 1H), 3.86 (s, 6H), 3.89−3.86 (m, 4H), 3.28 (appt, J = 4.88 Hz, 4H), 2.86 (s, 6H); ^{13}C NMR ($CDCl_3$) 172.0, 160.6, 78.5, 53.5, 46.2, 43.5, 38.2; EI-MS (m/z) 331 (M^+). Anal. Calcd for $C_{12}H_{21}N_5O_4S$: C, 43.49; H, 6.39; N, 21.13; S, 9.68. Found: C, 43.60; H, 6.47; N, 21.11; S, 9.85.

4-(5-Hydroxy-4,6-dimethoxypyrimidin-2-yl)-*N,N′*-dimethylpiperazine-1-sulfonamide (6). To a solution of compound **5** (1.66 g, 5 mmol) in 40 mL of THF at −78 °C and under an Ar atmosphere was added 0.3 mL of *n*-BuLi (7 mmol). After the mixture was stirred for 3 h at −60 °C, the Ar atmosphere was replaced with oxygen. The reaction mixture was then gradually warmed to room temperature (RT), and stirring was continued for an additional 6 h. After adjusting the pH to 6−7 with dilute HCl, THF was removed by evaporation and the remaining aqueous layer was extracted with $CHCl_3$. The $CHCl_3$ layers were washed with brine, dried over Na_2SO_4, and filtered. Solvent evaporation gave a yellow solid, which was purified by CC with 1:1:2 $CHCl_3$/EtOAc/hexane to yield 530 mg (30%) of compound **6**, mp 113−114 °C. The structure was confirmed by ^{1}H NMR ($CDCl_3$) δ 4.21 (s, 1H), 3.95 (s, 6H), 3.76 (s, 4H), 3.29 (s, 4H), 2.86 (s, 6H); EI-MS (m/z) 347 (M^+). Anal. Calcd for $C_{12}H_{21}N_5O_5S$: C, 41.49; H, 6.09; N, 21.16; S, 9.23. Found: C, 43.61; H, 6.13; N, 19.96; S, 9.18.

***N,N*-Dimethyl-4-(5-nitropyrimidin-2-yl)piperazine-1-sulfonamide (16).** Triethylamine (7.2 mL, 51.8 mmol) was added to a solution of **10** (10 g, 51.8 mmol) dissolved in 400 mL of THF. 2-Chloro-5-nitropyrimidine **12** (7.7 g, 48.3 mmol) dissolved in 20 mL of THF was added to the stirred mixture. After the mixture was stirred for 24 h at RT, THF was removed under vacuum and 600 mL of $CHCl_3$ was added to the residue. The $CHCl_3$ layer was washed with 0.5 N HCl, water, and brine, dried over Na_2SO_4, and filtered. Solvent evaporation gave 14.1 g (92%) of straw-yellow solid **16**. ^{1}H NMR ($CDCl_3$) δ 9.08 (s, 2H), 4.09 (appt, J = 5.13 Hz, 4H), 3.35 (appt, J = 5.13 Hz, 4H), 2.87 (s, 6H).

4-(5-Aminopyrimidin-2-yl)-*N,N*-dimethylpiperazine-1-sulfonamide (17). NH_4Cl (1.43 g, 26.76 mmol) was added to a suspension of **16** (14.1 g, 44.6 mmol) in a mixture of EtOH (175 mL) and

H_2O (48 mL), followed by iron powder (7.5 g, 133.9 mmol). After refluxing 1 h, the reaction mixture was filtered and concentrated to give a brown solid which was dissolved in 800 mL of $CHCl_3$, washed with $NaHCO_3$ and brine, dried over Na_2SO_4, and filtered. Solvent evaporation gave a yellow solid which after CC with 100:1 $CHCl_3$/MeOH gave 11.5 g (90%) of solid yellow **17**. ^{1}H NMR ($CDCl_3$) δ 7.98 (s, 2H), 3.76 (t, J = 4.88 Hz, 4H), 3.30 (t, J = 4.88 Hz, 4H), 2.86 (s, 6H); EI-MS (m/z) 286 (M^+).

4-(5-Hydroxypyrimidin-2-yl)-*N*,*N*-dimethylpiperazine-1-sulfonamide (2). A suspension of **17** (5.76 g, 20.2 mmol) in 100 mL of 2 M H_2SO_4 was refluxed for 1.5 h until the suspension became clear. After the mixture was cooled to RT, the solution pH was adjusted to 6−7 with 10 N NaOH, and the cloudy mixture was extracted with EtOAc. The combined organic layers were washed with brine, dried over Na_2SO_4, and filtered. Solvent evaporation gave a yellow solid, which was purified by CC using 1:1 EtOAc/hexane to yield 3.23 g (56%) of white solid compound **2**, mp 134−135 °C. ^{1}H NMR ($CDCl_3$) δ 8.08 (s, 2H), 3.78 (appt, J = 5.13 Hz, 4H), 3.29 (appt, J = 5.13 Hz, 4H), 2.86 (s, 6H); ^{13}C NMR ($CDCl_3$) 156.9, 145.8, 143.5, 46.0, 44.3, 38.1; EI-MS (m/z) 287 (M^+). Anal. Calcd for $C_{10}H_{17}N_5O_3S$: C, 41.80; H, 5.96; N, 24.37; S, 11.16. Found: C, 41.60; H, 5.98; N, 24.16; S, 11.02.

5-Hydroxy-2-aminopyrimidine (25). Under argon at RT, BBr_3 (2.6 mL, 50 mmol) was added dropwise to a solution of **23** (1.25 g, 10 mmol) in 60 mL of benzene, and the mixture was refluxed for 6 h. After the mixture stood overnight at RT, the solvent was evaporated and the residue was carefully treated with 10 mL of ice cold H_2O. The pH of the solution was adjusted to 6−7 with 6 N NaOH and then extracted with EtOAc. The EtOAc layers were washed with brine, dried over Na_2SO_4, and filtered. Solvent evaporation gave a yellow solid, which after CC using 20:1 $CHCl_3$/MeOH gave 840 mg (75%) of white solid 5-hydroxy-2-aminopyrimidine **25**. ^{1}H NMR (DMSO-d_6) δ 8.90 (s, 1H), 7.86 (s, 2H), 5.91 (s, 2H); EI-MS (m/z) 111 (M^+).

5-Benzyloxy-2-aminopyrimidine (20c). K_2CO_3 (276 mg, 2 mmol) was added to 222 mg of **25** (2 mmol) in 5 mL of methanol, followed by BnBr (0.24 mL, 2 mmol). After the mixture was stirred for 14 h at RT, the reaction was stopped by addition of water. Methanol was evaporated. The remaining aqueous layer was extracted with $CHCl_3$. The combined $CHCl_3$ layers were washed with brine, dried over Na_2SO_4, and filtered. Removal of the solvent followed by CC using 67:1 $CHCl_3$/MeOH yielded 300 mg (75%) of white solid **20c**. ^{1}H NMR ($CDCl_3$) δ 8.08 (s, 2H), 7.40−7.32 (m, 5H), 5.03 (s, 2H), 4.77 (br s, 2H).

2-Chloro-5-hydroxy-4,6-dimethoxypyrimidine (28). To a stirred suspension of 10.44 g 2-chloro-4,6-dimethoxypyrimidine **11b**, (60 mmol) in 200 mL of THF under argon at −78 °C was added dropwise a solution of LDA (2 M in THF/heptane/ethyl benzene, 60 mL, 120 mmol). To a separate round-bottomed flask at −78 °C under argon containing *tert*-butyl hydroperoxide (5.5 M in decane, 22.7 mL,125 mmol) in 150 mL of THF was added a solution of *n*-BuLi (1.6 M in hexane, 78 mL, 125 mmol). Then, after being stirred for 1 h, the hydroperoxide anion solution was added via a double-ended needle to the aromatic anion. The temperature was gradually raised to 0 °C, with stirring continuing an additional 3 h. The reaction was quenched with 6 N HCl until a pH of 7 was obtained. After THF evaporation the remaining aqueous layer was extracted with $CHCl_3$. The $CHCl_3$ layers were washed with brine, dried over Na_2SO_4, and filtered. Removal of solvent and subsequent purification by CC using 100:1 $CHCl_3$/MeOH gave 10.67 g (93.4%) of white solid **28**. ^{1}H NMR ($CDCl_3$) δ 4.93 (s, 1H), 4.05 (s, 6H); ^{13}C NMR ($CDCl_3$) 158.1, 146.7, 123.0, 55.1.

2-Chloro-5-(benzyloxy)-4,6-dimethoxypyrimidine (29). K_2CO_3 (10.0 g, 70 mmol) was added to **28** (13.24 g, 69.5 mmol) dissolved in 200 mL of MeCN followed by BnBr (8.3 mL, 69.5 mmol). After the mixture was stirred for 14 h at RT, the reaction was stopped by addition of water. MeCN was evaporated, the remaining aqueous layer was extracted with $CHCl_3$. The combined $CHCl_3$ layers were washed with brine, dried over Na_2SO_4, and filtered. Removal of the solvent followed by CC using 25:1 hexane/EtOAc gave 16.57 g (85%) of benzyloxy **29**. ^{1}H NMR ($CDCl_3$) δ 7.41−7.31 (m, 5H), 5.00 (s, 2H), 3.98 (s, 6H); ^{13}C NMR ($CDCl_3$) 163.6, 150.5, 136.4, 128.5, 128.4, 128.3, 124.4, 74.8, 54.0.

***N*-Benzyl-5-(benzyloxy)-4,6-dimethoxypyrimidin-2-amine (30).** A mixture of **29** (3.18 g, 11.33 mmol), $BnNH_2$ (2.2 mL, 20 mmol), and K_2CO_3 (1.66 g, 12 mmol) in dioxane (60 mL) was refluxed for 4 days. The mixture was filtered and the filtrate concentrated in vacuo to give a yellow oil, which after CC with 25:1 to 10:1 hexane/EtOAc gave 2.54 g (64%) of white solid **30**. ^{1}H NMR ($CDCl_3$) δ 7.45−7.24 (m, 10H), 5.10 (br s, 1H), 4.85 (s, 2H), 4.55 (d, J = 5.5 Hz, 2H), 3.86 (s, 6H); ^{13}C NMR ($CDCl_3$) 163.5, 156.0, 139.7, 137.5, 128.5, 128.4, 128.1, 127.8, 127.6, 127.1, 117.7, 75.2, 53.7, 45.9.

2-Amino-4,6-dimethoxypyrimidin-5-ol (31). Compound **30** (2.54 g, 7.24 mmol) in 40 mL of MeOH was hydrogenated for 12 h at RT in the presence of 635 mg of 10% Pd/C catalyst. After filtration and solvent evaporation, a white solid was obtained, which after CC using 50:1 $CHCl_3$/MeOH yielded 1.21 g (98%) of **31**. ^{1}H NMR ($CDCl_3$) δ 4.50 (s, 2H), 4.30 (s, 1H), 3.93 (s, 6H).

5-(Benzyloxy)-4,6-dimethoxypyrimidin-2-amine (20d). To 4.16 g of **31** (24.3 mmol) in MeOH (240 mL) was added K_2CO_3 (3.5 g, 25 mmol), followed by BnBr (3.0 mL, 25 mmol). After the mixture was stirred for 12 h at RT, water was added to the reaction mixture. MeOH was evaporated, and the water layer was extracted with $CHCl_3$. The combined $CHCl_3$ layers were washed with brine, dried over Na_2SO_4, and filtered. Removal of $CHCl_3$ gave a yellow solid, which after purification by CC with 10:1 to 2:1 hexane/EtOAc yielded 5.14 g (81%) of 2-amine-4,6-dimethoxy-5-benzyloxypyrimidine **20d**. ^{1}H NMR ($CDCl_3$) δ 7.44−7.27 (m, 5H), 4.86 (s, 2H), 4.60 (s, 2H), 3.87 (s, 6H).

2,2′-(*N*,*N*-Dimethylsulfamoylazanediyl)diacetic Acid (19). An amount of 26.62 g of the iminodiacetic acid **18** (200 mmol) was added to 16.0 g of NaOH (400 mmol) in 50 mL of H_2O at 0 °C, followed by 21.2 g of Na_2CO_3 (200 mmol) in 100 mL of H_2O. Then dimethylsulfamoyl chloride (200 mmol) dissolved in 50 mL of acetone was slowly added with stirring and the stirring was continued at RT. After 48 h, the reaction mixture was extracted with EtOAc. The pH of the aqueous layer was adjusted to 2 with 12 N HCl and extracted again with EtOAc. The organic layer was dried over Na_2SO_4 and filtered. Solvent evaporation gave 28.75 g (60%) of **19** as a white powder which was recrystallization from EtOAc. The structure was confirmed by ^{1}H NMR (DMSO-d_6) δ 12.81 (br s, 2H), 3.99 (s, 4H), 2.71 (s, 6H); ^{13}C NMR (DMSO-d_6) 170.9, 49.7, 37.8.

General Procedure for Preparation of *N*,*N*′-Dimethyl-3,5-dioxo-4-(pyrimidin-2-yl)piperazine-1-sulfonamide (3), 4-(4,6-Dimethoxypyrimidin-2-yl)-*N*,*N*-dimethyl-3,5-dioxopiperazine-1-sulfonamide (7), 4-(5-(Benzyloxy)pyrimidin-2-yl)-*N*,*N*-dimethyl-3,5-dioxopiperazine-1-sulfonamide (21), and 4-(5-(Benzyloxy)-4,6-dimethoxypyrimidin-2-yl)-*N*,*N*-dimethyl-3,5-dioxopiperazine-1-sulfonamide (22). A suspension of 1.44 g of diacid **19** (6 mmol) in 8.0 mL of Ac_2O was heated to 85 °C for 5 min until the solution became clear. After excess Ac_2O was removed under vacuum at 60 °C, the resulting anhydride was obtained as a yellow oil. The resulting anhydride, in 10 mL of toluene, was then reacted with 475 mg of 2-aminopyrimidine **20a** (5 mmol) dissolved in 7 mL of acetone by heating the mixture to 80 °C for 6 h. Solvent evaporation gave the amide as a yellow oil. Heating amide for 4 h at 80 °C with 8 mL of Ac_2O resulted into the final piperidine-2,6-ring product as a red, clear solution. Removal of the remaining Ac_2O under vacuum at 60 °C followed by CC with 3:1:1 hexane/EtOAc/$CHCl_3$ gave 760 mg (50.8%) of compound **3**, mp 179−181 °C. ^{1}H NMR ($CDCl_3$) δ 8.90 (d, J = 4.88 Hz, 2H), 7.45 (t, J = 4.88 Hz, 1H), 4.31 (s, 4H), 2.96 (s, 6H); ^{13}C NMR ($CDCl_3$) 167.0, 159.5, 154.8, 121.4, 49.5, 38.3; ESI-MS (m/z) 322 ([M + Na]$^+$). Anal. Calcd for $C_{10}H_{13}N_5O_4S$: C, 40.13; H, 4.38; N, 23.40; S, 10.71. Found: C, 40.40; H, 4.54; N, 23.41; S, 10.66.

The white solid of compound **7**, mp 200−202 °C, was obtained in 57.9% yield. ^{1}H NMR ($CDCl_3$) δ 6.10 (s, 1H), 4.30 (s, 4H), 3.92

(s, 6H), 2.967 (s, 6H); ^{13}C NMR ($CDCl_3$) 172.8, 166.7, 152.8, 90.5, 54.7, 49.4, 38.2; ESI-MS (m/z) 382 ($[M + Na]^+$). Anal. Calcd for $C_{12}H_{17}N_5O_6S$: C, 40.11; H, 4.77; N, 19.49; S, 8.92. Found: C, 40.31; H, 4.84; N, 19.28; S, 9.10.

Crude compound **21** was purified by CC with 100:1 $CHCl_3$/MeOH, and white solid of **21** was obtained in 69% yield. ^{1}H NMR ($CDCl_3$) δ 8.56 (s, 2H), 7.44−7.26 (m, 5H), 5.20 (s, 2H), 4.29 (s, 4H), 2.95 (s, 6H).

Crude compound **22** was purified by CC using 100:1 $CHCl_3$/MeOH, and pale-yellow solid of **22** was obtained in 41% yield. ^{1}H NMR ($CDCl_3$) δ 7.46−7.32 (m, 5H), 5.05 (s, 2H), 4.29 (s, 4H), 3.95 (s, 6H), 2.96 (s, 6H).

General Procedure for Preparation of 4-(5-Hydroxypyrimidin-2-yl)-*N*,*N*-dimethyl-3,5-dioxopiperazine-1-sulfonamide (4) and 4-(5-Hydroxy-4,6-dimethoxypyrimidin-2-yl)-*N*,*N*-dimethyl-3,5-dioxopiperazine-1-sulfonamide (8). Compound **21** (2.0 g, 4.9 mmol) dissolved in 100 mL of EtOAc was hydrogenated with 500 mg of 10% Pd/C catalyst at RT for 12 h. After filtration and solvent evaporation, compound **4** recrystallized from EtOAc to give 1.83 g (80%) of a white powder, mp 225−226 °C. ^{1}H NMR (DMSO-d_6) δ 11.0 (s, 1H), 8.45 (s, 2H), 4.39 (s, 4H), 2.85 (s, 6H); ^{13}C NMR ($CDCl_3$) 168.9, 152.7, 146.9, 146.1, 50.0, 38.5; ESI-MS (m/z) 338 ($[M + Na]^+$). Anal. Calcd for $C_{10}H_{13}N_5O_5S$: C, 38.09; H, 4.16; N, 22.21; S, 10.17. Found: C, 38.18; H, 4.35; N, 21.98; S, 9.93.

Crude compound **8** was purified by CC using 80:1 $CHCl_3$/MeOH to yield 1.15 g (91%) of white solid **8**, mp 222−224 °C. ^{1}H NMR ($CDCl_3$) δ 9.67 (s, 1H), 4.44 (s, 4H), 3.88 (s, 6H), 2.51 (s, 6H); ^{13}C NMR ($CDCl_3$) 168.1, 159.4, 140.9, 124.7, 54.7, 49.3, 37.9; ESI-MS (m/z) 398 ($[M + Na]^+$). Anal. Calcd for $C_{12}H_{17}N_5O_7S$: C, 38.40; H, 4.56; N, 18.66; S, 8.54. Found: C, 38.60; H, 4.66; N, 18.49; S, 8.58.

Chelation Studies. The relative amounts of ions bound by compounds **1**−**8** were determined by electrospray ionization mass spectrometry (ESI-MS) according to the method of Baron and Hering.[71] Stock solutions (1 mM) were prepared with doubly distilled water from ammonium iron(II) sulfate hexahydrate, iron(III) nitrate nonahydrate, copper(I) chloride, copper(II) chloride dihydrate, zinc chloride, magnesium chloride, and calcium chloride. Each ion solution was mixed with compounds **1**−**8**, respectively, in ratios of 10:1, 1:1, and 1:10 metal ion/compound so that a final compound concentration of 50 μM was maintained. Forty-five minutes after mixing, each solution was directly infused into the MS under constant ionization energy.

The stoichiometry of the complexes of compounds **1**−**8** with Fe^{2+}, Fe^{3+}, Cu^{1+}, Cu^{2+}, Zn^{2+}, Ca^{2+}, and Mg^{2+} was determined using the method of continuous variation (Job plots).[72] Because of their low solubility, compounds **1**−**8** were first dissolved in acetonitrile (HPLC grade). These concentrated solutions were then diluted to 0.1 mM stock solutions with 1 mM acetate (pH 6.5). In a typical experiment (at 23 °C), several solutions of the compound and metal ion of interest were prepared at a constant total concentration of compound and ion but with a different mole fraction of one component. After an equilibration period of 45 min, the change in UV absorbance was monitored from 210 to 310 nm. The maximum absorbance for each compound was then recorded as a function of the mole fraction of the metal ion. Two linear dependences were obtained, at low and high molar fractions, which intersect at a mole fraction value that corresponds to the stoichiometry of the complex.

Cell Culture Studies. Human lens epithelial cells (SRA-1), obtained as a gift from Dr. Reddy,[69] were cultured in Dulbecco's modified Eagle's medium (DMEM) containing 10% fetal bovine serum (FBS), 4 mM L-glutamine, 1.5 g/L $NaHCO_3$, and 1% penicillin/streptomycin solution. Human retinal pigmented epithelial cells (ARPE-19), obtained from the American Type Culture Collection (Manassas, VA), were cultured in a 1:1 mixture of Dulbecco's modified Eagle's medium and Ham's F12 (DMEM/F12) medium with 2.5 mM L-glutamine and 15 mM HEPES buffer (Gibco, Carlsbad, CA) containing 10% heat-inactivated FBS and 1% penicillin/streptavidin solution. Human hippocampal astrocytes (HA-h), obtained from the ScienCell Research Laboratories (Carlsbad, CA), were cultured on poly-L-lysine coated containers (2 μg/cm^2) with astrocyte medium (ScienCell, Carlsbad, CA) composed of 500 mL of basal medium, 5 mL of astrocyte growth supplement, and 5 mL of penicillin/streptomycin solution. All cells were cultured at 37 °C in a humidified atmosphere of 5% CO_2 and 95% air until subconfluent (2−4 days). Cells were passaged when 80−90% confluent by treatment with trypsin−EDTA and then plated at a density of 1×10^4 cells onto 96-well plates or 1×10^6 cells onto 150 mm dishes. For compound evaluation, FBS-free media (blank and control) or FBS-free media containing either 100 μM compounds **1**−**8** or 100 μM water-soluble vitamin E analogue 6-hydroxy-2,5,7,8-tetramethylchroman-2-carboxylic acid (Trolox) were added to each individual well/dish. After 1 h, an additional aliquot of FBS-free media was added to the blank well/dish, and a similar volume of FBS-free media containing 1 mM H_2O_2 was added to all remaining wells/dishes. For the Fenton studies, addition of H_2O_2 was immediately followed by addition of 1 mM ammonium iron(II) sulfate hexahydrate. After 2 h of exposure, all media were removed and the cells were washed at room temperature with PBS. All studies were conducted in triplicate.

Cell viability studies were conducted in 96-well plates using the CellTiter 96 AQueous One Solution Cell Proliferation Assay (MTS, Promega, Madison, WI). Briefly, after 2 h of exposure to either H_2O_2 or Fenton reagents, media were removed from all wells and each well was washed with PBS. After removal of the PBS wash, 100 μL of blank media was added to each well followed by addition of 20 μL of the MTS solution. The cells were further incubated at 37 °C for 1.5 h and then spectrophotometrically evaluated at 490 nm in a plate reader. The results were normalized to blank control (100%) of cells not treated with H_2O_2.

GSH measurements were conducted on cells cultured in either 100 or 150 mm dishes. After 2 h of exposure to either H_2O_2 or Fenton reagents, the media were removed and the cells were washed with PBS. The cells were removed from each dish by scraping and homogenized in glass homogenizers. Following centrifugation at 4 °C, protein levels in the supernatant were measured according to Bradford.[73] The cell homogenates were then deproteinized with equal volumes of 20% trichloroacetic acid (TCA), and GSH levels were measured at 412 nm according to the DTNB method.[74] GSH levels were expressed as nmol of GSH/mg of protein, with values subsequently normalized to GSH levels in cells not exposed to H_2O_2 (blank control, 100%).

Acknowledgment. This work was supported by National Institutes of Health Grant EY016460.

References

(1) Brewer, G. J. Iron and copper toxicity in diseases of aging, particularly atherosclerosis and Alzheimer's disease. *Exp. Biol. Med.* (*Maywood, NJ, U. S.*) **2007**, *232*, 323–335.
(2) Gilca, M.; Stoian, I.; Atanasiu, V.; Virgolici, B. The oxidative hypothesis of senescence. *J. Postgrad. Med.* **2007**, *53*, 207–213.
(3) Stadtman, E. R.; Oliver, C. N.; Levine, R. L.; Fucci, L.; Rivett, A. J. Implication of protein oxidation in protein turnover, aging, and oxygen toxicity. *Basic Life Sci.* **1988**, *49*, 331–339.
(4) Allsop, D.; Mayes, J.; Moore, S.; Masad, A.; Tabner, B. J. Metal-dependent generation of reactive oxygen species from amyloid proteins implicated in neurodegenerative disease. *Biochem. Soc. Trans.* **2008**, *36*, 1293–1298.
(5) Smith, D. G.; Cappai, R.; Barnham, K. J. The redox chemistry of the Alzheimer's disease amyloid beta peptide. *Biochim. Biophys. Acta* **2007**, *1768*, 1976–1990.
(6) Valko, M.; Morris, H.; Cronin, M. T. Metals, toxicity and oxidative stress. *Curr. Med. Chem.* **2005**, *12*, 1161–1208.
(7) Brennan, L. A.; Kantorow, M. Mitochondrial function and redox control in the aging eye: role of MsrA and other repair systems in cataract and macular degenerations. *Exp. Eye Res.* **2009**, *88*, 195–203.

(8) Dunaief, J. L.; Richa, C.; Franks, E. P.; Schultze, R. L.; Aleman, T. S.; Schenck, J. F.; Zimmerman, E. A.; Brooks, D. G. Macular degeneration in a patient with aceruloplasminemia, a disease associated with retinal iron overload. *Ophthalmology* **2005**, *112*, 1062–1065.

(9) Richer, S.; Rudy, D.; Statkute, L.; Karofty, K.; Frankowski, J. Serum iron, transferrin saturation, ferritin, and dietary data in age-related macular degeneration. *Am. J. Ther.* **2002**, *9*, 25–28.

(10) Dunaief, J. L. Iron induced oxidative damage as a potential factor in age-related macular degeneration: the Cogan lecture. *Invest. Ophthalmol. Visual Sci.* **2006**, *47*, 4660–4664.

(11) Garner, B.; Roberg, K.; Qian, M.; Brunk, U. T.; Eaton, J. W.; Truscott, R. J. Redox availability of lens iron and copper: implications for HO* generation in cataract. *Redox Rep.* **1999**, *4*, 313–315.

(12) Ecroyd, H.; Carver, J. A. Crystallin proteins and amyloid fibrils. *Cell. Mol. Life Sci.* **2009**, *66*, 62–81.

(13) Narayanan, S.; Kamps, B.; Boelens, W. C.; Reif, B. alphaB-crystallin competes with Alzheimer's disease beta-amyloid peptide for peptide-peptide interactions and induces oxidation of Abeta-Met35. *FEBS Lett.* **2006**, *580*, 5941–5946.

(14) Lee, S.; Carson, K.; Rice-Ficht, A.; Good, T. Hsp20, a novel alpha-Crystallin, prevents Abeta fibril formation and toxicity. *Protein Sci.* **2005**, *14*, 593–601.

(15) Smith, D. G.; Cappai, R.; Barnham, K. J. The redox chemistry of the Alzheimer's disease amyloid beta peptide. *Biochim. Biophys. Acta* **2007**, *1768*, 1976–1990.

(16) Anderson, D. H.; Talaga, K. C.; Rivest, A. J.; Barron, E.; Hageman, G. S.; Johnson, L. V. Characterization of beta amyloid assemblies in drusen: the deposits associated with aging and age-related macular degeneration. *Exp. Eye Res.* **2004**, *78*, 243–256.

(17) Bruban, J.; Glotin, A. L.; Dinet, V.; Chalour, N.; Sennlaub, F.; Jonet, L.; An, N.; Faussat, A. M.; Mascarelli, F. Amyloid-beta-(1-42) alters structure and function of retinal pigmented epithelial cells. *Aging Cell* **2009**, *8*, 162–177.

(18) Wang, J.; Ohno-Matsui, K.; Yoshida, T.; Shimada, N.; Ichinose, S.; Sato, T.; Mochizuki, M.; Morita, I. Amyloid-beta up-regulates complement factor B in retinal pigment epithelial cells through cytokines released from recruited macrophages/microglia: another mechanism of complement activation in age-related macular degeneration. *J. Cell. Physiol.* **2009**, *220*, 119–128.

(19) Surolia, I.; Sinha, S.; Sarkar, D. P.; Reddy, P. Y.; Reddy, G. B.; Surolia, A. Concurrence of Danish dementia and cataract: insights from the interactions of dementia associated peptides with eye lens alpha-crystallin. *PLoS One* **2008**, *3*, No. e2927.

(20) Goldstein, L. E.; Muffat, J. A.; Cherny, R. A.; Moir, R. D.; Ericsson, M. H.; Huang, X.; Mavros, C.; Coccia, J. A.; Faget, K. Y.; Fitch, K. A.; Masters, C. L.; Tanzi, R. E.; Chylack, L. T., Jr.; Bush, A. I. Cytosolic beta-amyloid deposition and supranuclear cataracts in lenses from people with Alzheimer's disease. *Lancet* **2003**, *361*, 1258–1265.

(21) Meehan, S.; Berry, Y.; Luisi, B.; Dobson, C. M.; Carver, J. A.; MacPhee, C. E. Amyloid fibril formation by lens crystallin proteins and its implications for cataract formation. *J. Biol. Chem.* **2004**, *279*, 3413–3419.

(22) Frank, B.; Gupta, S. A review of antioxidants and Alzheimer's disease. *Ann. Clin. Psychiatry* **2005**, *17*, 269–286.

(23) Garcia-Arencibia, M.; Gonzalez, S.; de Lago, E.; Ramos, J. A.; Mechoulam, R.; Fernandez-Ruiz, J. Evaluation of the neuroprotective effect of cannabinoids in a rat model of Parkinson's disease: importance of antioxidant and cannabinoid receptor-independent properties. *Brain Res.* **2007**, *1134*, 162–170.

(24) Bolognesi, M. L.; Minarini, A.; Tumiatti, V.; Melchiorre, C. Lipoic acid, a lead structure for multi-target-directed drugs for neurodegeneration. *Mini-Rev. Med. Chem.* **2006**, *6*, 1269–1274.

(25) Binienda, Z.; Przybyla-Zawislak, B.; Virmani, A.; Schmued, L. L-Carnitine and neuroprotection in the animal model of mitochondrial dysfunction. *Ann. N.Y. Acad. Sci.* **2005**, *1053*, 174–182.

(26) Tauskela, J. S. MitoQ—a mitochondria-targeted antioxidant. *IDrugs* **2007**, *10*, 399–412.

(27) Perluigi, M.; Joshi, G.; Sultana, R.; Calabrese, V.; De Marco, C.; Coccia, R.; Butterfield, D. A. In vivo protection by the xanthate tricyclodecan-9-yl-xanthogenate against amyloid beta-peptide (1-42)-induced oxidative stress. *Neuroscience* **2006**, *138*, 1161–1170.

(28) Skulachev, V. P.; Anisimov, V. N.; Antonenko, Y. N.; Bakeeva, L. E.; Chernyak, B. V.; Erichev, V. P.; Filenko, O. F.; Kalinina, N. I.; Kapelko, V. I.; Kolosova, N. G.; Kopnin, B. P.; Korshunova, G. A.; Lichinitser, M. R.; Obukhova, L. A.; Pasyukova, E. G.; Pisarenko, O. I.; Roginsky, V. A.; Ruuge, E. K.; Senin, I. I.; Severina, I. I.; Skulachev, M. V.; Spivak, I. M.; Tashlitsky, V. N.; Tkachuk, V. A.; Vyssokikh, M. Y.; Yaguzhinsky, L. S.; Zorov, D. B. An attempt to prevent senescence: a mitochondrial approach. *Biochim. Biophys. Acta* **2009**, *1787*, 437–461.

(29) Gupta, S. K.; Selvan, V. K.; Agrawal, S. S.; Saxena, R. Advances in pharmacological strategies for the prevention of cataract development. *Indian J. Ophthalmol.* **2009**, *57*, 175–183.

(30) Evans, J. Antioxidant supplements to prevent or slow down the progression of AMD: a systematic review and meta-analysis. *Eye (London, U. K.)* **2008**, *22*, 751–760.

(31) Evans, J. R.; Henshaw, K. Antioxidant Vitamin and Mineral Supplements for Preventing Age-Related Macular Degeneration. In *Cochrane Database Of Systematic Reviews* (*Online*); The Cochrane Collaboration: Oxford, U.K., 2008; CD000253.

(32) House, E.; Collingwood, J.; Khan, A.; Korchazkina, O.; Berthon, G.; Exley, C. Aluminium, iron, zinc and copper influence the in vitro formation of amyloid fibrils of Abeta42 in a manner which may have consequences for metal chelation therapy in Alzheimer's disease. *J. Alzheimer's Dis.* **2004**, *6*, 291–301.

(33) CNS DRug DElivey. *NIH Monogram*; National Institutes of Health: Bethesda, MD.

(34) Wong, R. W.; Richa, D. C.; Hahn, P.; Green, W. R.; Dunaief, J. L. Iron toxicity as a potential factor in AMD. *Retina* **2007**, *27*, 997–1003.

(35) Avunduk, A. M.; Yardimci, S.; Avunduk, M. C.; Kurnaz, L. Cataractous changes in rat lens following cigarette smoke exposure is prevented by parenteral deferoxamine therapy. *Arch. Ophthalmol.* **1999**, *117*, 1368–1372.

(36) Melov, S.; Wolf, N.; Strozyk, D.; Doctrow, S. R.; Bush, A. I. Mice transgenic for Alzheimer disease beta-amyloid develop lens cataracts that are rescued by antioxidant treatment. *Free Radical Biol. Med.* **2005**, *38*, 258–261.

(37) Cuajungco, M. P.; Lees, G. J. Diverse effects of metal chelating agents on the neuronal cytotoxicity of zinc in the hippocampus. *Brain Res.* **1998**, *799*, 97–107.

(38) Finefrock, A. E.; Bush, A. I.; Doraiswamy, P. M. Current status of metals as therapeutic targets in Alzheimer's disease. *J. Am. Geriatr. Soc.* **2003**, *51*, 1143–1148.

(39) Clifford Rose, F.; Gawel, M. Clioquinol neurotoxicity: an overview. *Acta Neurol. Scand. Suppl.* **1984**, *100*, 137–145.

(40) Treiber, C.; Simons, A.; Strauss, M.; Hafner, M.; Cappai, R.; Bayer, T. A.; Multhaup, G. Clioquinol mediates copper uptake and counteracts copper efflux activities of the amyloid precursor protein of Alzheimer's disease. *J. Biol. Chem.* **2004**, *279*, 51958–51964.

(41) Raman, B.; Ban, T.; Yamaguchi, K.; Sakai, M.; Kawai, T.; Naiki, H.; Goto, Y. Metal ion-dependent effects of clioquinol on the fibril growth of an amyloid {beta} peptide. *J. Biol. Chem.* **2005**, *280*, 16157–16162.

(42) Jenagaratnam, L.; McShane, R. Clioquinol for the Treatment of Alzheimer's Disease. In *Cochrane Database of Systematic Reviews* (*Online*); The Cochrane Collaboration: Oxford, U.K., 2006.

(43) Crouch, P. J.; Barnham, K. J.; Bush, A. I.; White, A. R. Therapeutic treatments for Alzheimer's disease based on metal bioavailability. *Drug News Perspect.* **2006**, *19*, 469–474.

(44) Lannfelt, L.; Blennow, K.; Zetterberg, H.; Batsman, S.; Ames, D.; Harrison, J.; Masters, C. L.; Targum, S.; Bush, A. I.; Murdoch, R.; Wilson, J.; Ritchie, C. W. Safety, efficacy, and biomarker findings of PBT2 in targeting Abeta as a modifying therapy for Alzheimer's disease: a phase IIa, double-blind, randomised, placebo-controlled trial. *Lancet Neurol.* **2008**, *7*, 779–786.

(45) Adlard, P. A.; Cherny, R. A.; Finkelstein, D. I.; Gautier, E.; Robb, E.; Cortes, M.; Volitakis, I.; Liu, X.; Smith, J. P.; Perez, K.; Laughton, K.; Li, Q. X.; Charman, S. A.; Nicolazzo, J. A.; Wilkins, S.; Deleva, K.; Lynch, T.; Kok, G.; Ritchie, C. W.; Tanzi, R. E.; Cappai, R.; Masters, C. L.; Barnham, K. J.; Bush, A. I. Rapid restoration of cognition in Alzheimer's transgenic mice with 8-hydroxy quinoline analogs is associated with decreased interstitial Abeta. *Neuron* **2008**, *59*, 43–55.

(46) Kupershmidt, L.; Weinreb, O.; Amit, T.; Mandel, S.; Carri, M. T.; Youdim, M. B. Neuroprotective and neuritogenic activities of novel multimodal iron-chelating drugs in motor-neuron-like NSC-34 cells and transgenic mouse model of amyotrophic lateral sclerosis. *FASEB J.* **2009**, *23*, 3766–3779.

(47) Weinreb, O.; Mandel, S.; Bar-Am, O.; Yogev-Falach, M.; Avramovich-Tirosh, Y.; Amit, T.; Youdim, M. B. Multifunctional neuroprotective derivatives of rasagiline as anti-Alzheimer's disease drugs. *Neurotherapeutics* **2009**, *6*, 163–174.

(48) Silver, H.; Chertkow, Y.; Weinreb, O.; Danovich, L.; Youdim, M. Multifunctional pharmacotherapy: what can we learn from study of selective serotonin reuptake inhibitor augmentation of antipsychotics in negative-symptom schizophrenia? *Neurotherapeutics* **2009**, *6*, 86–93.

(49) Forni, G. L.; Balocco, M.; Cremonesi, L.; Abbruzzese, G.; Parodi, R. C.; Marchese, R. Regression of symptoms after selective iron

chelation therapy in a case of neurodegeneration with brain iron accumulation. *Movement Disord.* **2008**, *23*, 904–907.
(50) Kruck, T. P.; Burrow, T. E. Synthesis of feralex a novel aluminum/iron chelating compound. *J. Inorg. Biochem.* **2002**, *88*, 19–24.
(51) Kruck, T. P.; Percy, M. E.; Lukiw, W. J. Metal sulfate-mediated induction of pathogenic genes and repression by phenyl butyl nitrone and feralex-G. *NeuroReport* **2008**, *19*, 245–249.
(52) Brewer, G. J. The risks of free copper in the body and the development of useful anticopper drugs. *Curr. Opin. Clin. Nutr. Metab. Care* **2008**, *11*, 727–732.
(53) Lee, J. Y.; Friedman, J. E.; Angel, I.; Kozak, A.; Koh, J. Y. The lipophilic metal chelator DP-109 reduces amyloid pathology in brains of human beta-amyloid precursor protein transgenic mice. *Neurobiol. Aging* **2004**, *25*, 1315–1321.
(54) Scott, L. E.; Orvig, C. Medicinal inorganic chemistry approaches to passivation and removal of aberrant metal ions in disease. *Chem. Rev.* **2009**, *109*, 4885–4910.
(55) Bush, A. I.; Tanzi, R. E. Therapeutics for Alzheimer's disease based on the metal hypothesis. *Neurotherapeutics* **2008**, *5*, 421–432.
(56) Kador, P. F.; Jin, H. Multifunctional Compounds and Methods of Use Thereof. Patent Appl. 20090105269, **2009**.
(57) Kador, P. F.; Inoue, J.; Blessing, K. Anticataract activity of analogs of a sorbitol dehydrogenase inhibitor. *J. Ocul. Pharmacol. Ther.* **2004**, *20*, 333–344.
(58) Gino, A.; DiLabio, G. A.; Brigati, G.; Pedulli, G. F.; Valgimigli, L. 5-Pyrimidinols: novel chain-breaking antioxidants more effective than phenols. *J. Am. Chem. Soc.* **2001**, *123*, 4625–4626.
(59) Bakalbassis, E. G.; Lithoxoidou, A. T.; Vafiadis, A. P. Theoretical calculation of accurate absolute and relative gas- and liquid-phase O−H bond dissociation enthalpies of 2-mono- and 2,6-disubstituted phenols, using DFT/B3LYP. *J. Phys. Chem. A* **2003**, *107*, 8594–8606.
(60) Jinno, S.; Okita, T. Synthesis and structure−activity relationships of phaffiaol and related antioxidants. *Chem. Pharm. Bull.* **1998**, *46*, 1688–1694.
(61) Pedulli, G.; Franco, L. M. Thermochemical and kinetic studies of antioxidants. *Trends Org. Chem.* **2001**, *9*, 97–105.
(62) Zaidi, S. A.; Shahjahan, A.; Sharif, M.; Siddiqi, K. S. Transition metal complexes of 2-(*N*-succinimidyl)pyrimidine. Synthesis and reactivity. *Inorg. Met.-Org. Chem.* **1993**, *23*, 1571–1584.
(63) Fourmaintraux, E.; Depreux, P.; Lesieur, I. Synthesis of new phthalazinyl compounds as potential inhibitors of aldose reductase and sorbitol dehydrogenase. *Heterocycl. Commun.* **1999**, *33*, 313–316.
(64) Parker, K. A.; Koziski, K. A. Directed hydroxylation of aromatics. *J. Org. Chem.* **1987**, *51*, 674–676.
(65) Kizner, T. A.; Mikhaleva, M. A.; Serebryakova, E. S. Selective acid hydrolysis of 2-substituted-5-dimethylaminomethyleneaminopyrimidines to 5-amino-and 5-hydroxypyrimidines. *Chem. Heterocycl. Compd.* **1990**, *6*, 668–670.
(66) Henry, D. W. A. Facile synthesis of piperazines from primary amines (1). *J. Heterocycl. Chem.* **1966**, *3*, 503–511.
(67) Priewe, H.; Gutsche, K. 5-Alkoxy-2-aminopyrimidines. DE 1145622, **1963**.
(68) Julia, M.; Pfeuty-Saint Jalmes, V.; Ple, K.; Verpeaux, J.-N. Hydroxylation of carbanions with lithium *tert*-butyl peroxide acting as an oxenoid. *Bull. Soc. Chim. Fr.* **1996**, *133*, 15–24.
(69) Ibaraki, N.; Chen, S. C.; Lin, L. R.; Okamoto, H.; Pipas, J. M.; Reddy, V. N. Human lens epithelial cell line. *Exp. Eye Res.* **1998**, *67*, 577–585.
(70) Dunn, K. C.; Aotaki-Keen, A. E.; Putkey, F. R.; Hjelmeland, L. M. ARPE-19, a human retinal pigment epithelial cell line with differentiated properties. *Exp. Eye Res.* **1996**, *62*, 155–169.
(71) Baron, D.; Hering, J. G. Analysis of metal−EDTA complexes by electrospray mass. spectrometry. *J. Environ. Qual.* **1998**, *27*, 844–850.
(72) Huang, C. Y. Determination of binding stoichiometry by the continuous variation method: the Job plot. *Methods Enzymol.* **1982**, *87*, 509–525.
(73) Bradford, M. M. A rapid and sensitive method for the quantitation of microgram quantities of protein utilizing the principle of protein−dye binding. *Anal. Biochem.* **1976**, *72*, 248–254.
(74) Lou, M. F.; Dickerson, J. E., Jr. Protein−thiol mixed disulfides in human lens. *Exp. Eye Res.* **1992**, *55*, 889–896.